Electronic Supplementary Material (ESI) for Sustainable Energy & Fuels.
This journal is © The Royal Society of Chemistry 2019

ELECTRONIC SUPPLEMENTARY MATERIAL
Controlling strategies to maximize reliability of integrated photo-electrochemical devices exposed to realistic disturbances

Saurabh Tembhurne[1], Sophia Haussener[1,*]
[1]Laboratory of Renewable Energy Science and Engineering, EPFL, Station 9, 1015 Lausanne, Switzerland

S.0 Degradation Modelling

The degradation of the concentrator is given by the decrease of the effective concentration of the concentrator. The degradation of the PV is modeled by an approach of an effective PV concentration. The time-dependent concentration profiles for the concentrator and PV [1] are shown in Fig. S.2. For the electrolyzer, the report by Fouda-Onana [2] was used to identify the main degradation phenomena. After various parametric analysis we identified three parameters in our EC model to mimic this degradation behavior. The variation of the ECs *J-V* curves with these parameters is shown in Fig. S.1a-c. The current density in the saturation region increases with an increase in the H^+ diffusion coefficient in the electrolyte membrane, hence, it was used to model the decrease in the EC's saturation current with time. With an increase in the gas diffusion layer's conductivity, the ohmic losses decrease. This effect is more pronounced at low conductivity values, making the GDL conductivity an ideal parameter to model the increase in ohmic losses and specifically to capture the high EC's efficiency losses at high current [2]. Similarly, the exchange current density of the anode/cathode (i.e. $IrRuO_2$ /Pt) was used to model the increase in the activation over-potential with time.

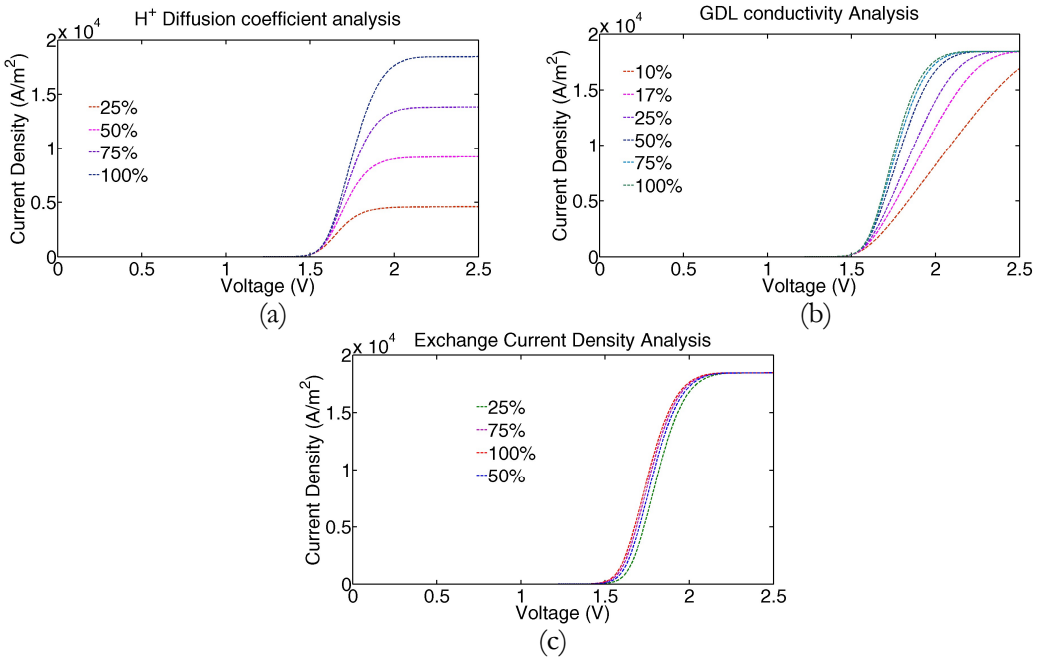

Fig. S.1 Current density versus potential characteristics for the integrated EC for variations (with respect to reference case, table S.1) in a) the H^+ diffusion coefficient in the electrolyte membrane, b) the GDLs conductivity, and c) the anode and cathode exchange current densities.

* Corresponding author: sophia.haussener@epfl.ch (+41 21 69 33878)

The reference degradation profiles of the parameters used for the analysis are shown in Fig. S.2, with the corresponding equations presented in table S.1. These rates are used in the manuscript, unless otherwise mentioned. Higher and medium degradation rate analysis are also presented which are based on the degradation profiles presented in Fig. S.2. For the medium case, the degradation rates are slightly higher (α =1.5) and for the higher case, they are significantly higher (α = 2) than the rates for the reference case. Table S.1 shows the corresponding equations and comparisons between the reference, medium, and higher degradation cases.

Table S.1 Description of the reference, medium and higher degradation profiles used for the degradation analysis.

Component degradation	**Degradataion modeling parameter**	**Parameter's equation**	α		
			Reference degradation	**Medium degradation**	**High degradation**
Concentrator	Concentration	$C_{new} = C(1\text{-}\alpha\ 0.0065\ \text{years})$	1	1.5	2
PV	Concentration	$C_{PV\_new} = C_{new}(1\text{-}\alpha\ 0.01\ \text{years})$	1	1.5	2
EC	H^+ diffusion coefficient	$D_{new} = D(1\text{-}\alpha\ 0.1\ \text{years}/3)$	1	1.5	2
	GDL conductivity	$\sigma^{GDL}_{new} = \sigma^{GDL}(1\text{-}\alpha\ (-0.002\ \text{years}^2 + 0.0734\ \text{years}))$	1	1.5	2
	Exchange current density	$J_{new} = J(1\text{-}\alpha\ 0.1\ \text{years}/3)$	1	1.5	2

The reference value of D is $2.4\text{x}10^{-5}$ [cm^2/s] , σ^{GDL} is 222 [S/m] and J are $4.62\cdot\exp(-48600/\bar{R}T)$ (anode-IrO_2), $142.02\cdot\exp(-28900/\bar{R}T)$ (cathode-Pt) [A/m^2].

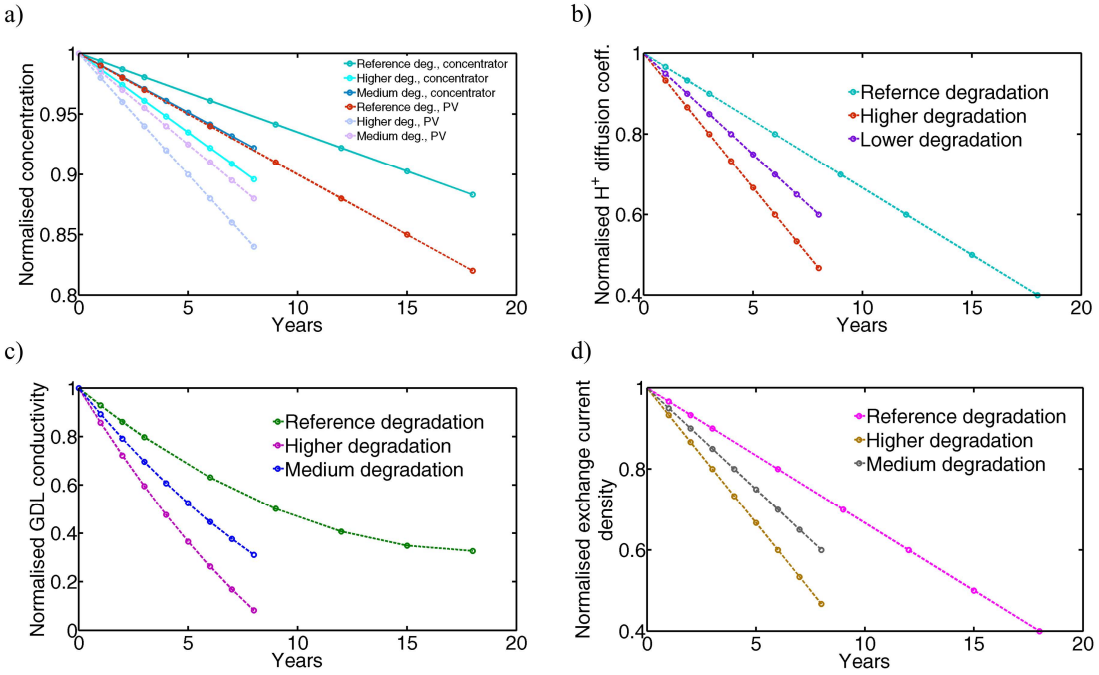

Fig. S.2 Degradation rate profiles of a) the effective concentration of the concentrator and of the PV, b) the H^+ diffusion coefficient in the electrolyte membrane, c) the GDL conductivity, and d) the anode-cathode exchange current densities, for the reference, medium, and high degradation cases.

For all the analyzed cases, the operating temperature is maintained below 80°C, hence we have an operation with liquid water and no polymeric electrolyte membrane dry out. We analyzed two types of semiconductor materials for the PV component. We define a triple junction thin film aSi-ucSi-ucSi cell based IPEC device which has a p-n-cathodic-anodic configuration to be the reference case I, and a dual junction III-V based $Ga_{0.51}In_{0.19}P$-GaAs cell based IPEC device which has a n-p-anodic-cathodic configuration to be reference case II. The input to the PV is assumed to come from a concentrator with an AM1.5G spectrum. Details about the spectral sampling are presented in Tembhurne et al.[3].

S.1 Mass flow rate: An integral parameter for thermal management

As discussed in detail in the manuscript, the variations of the mass flow rate of water causes the *J-V* curves of the EC to intersect in a small potential region which gives rise to two characteristic regions of operation[4]. These two distinctive zones (region I and II) and their formation is shown in Fig. S.3a-b which shows the *J-V* curves for varying water flow velocities for aSi-ucSi-ucSi (reference case I) and GaInP-GaAs (reference case II) based device.

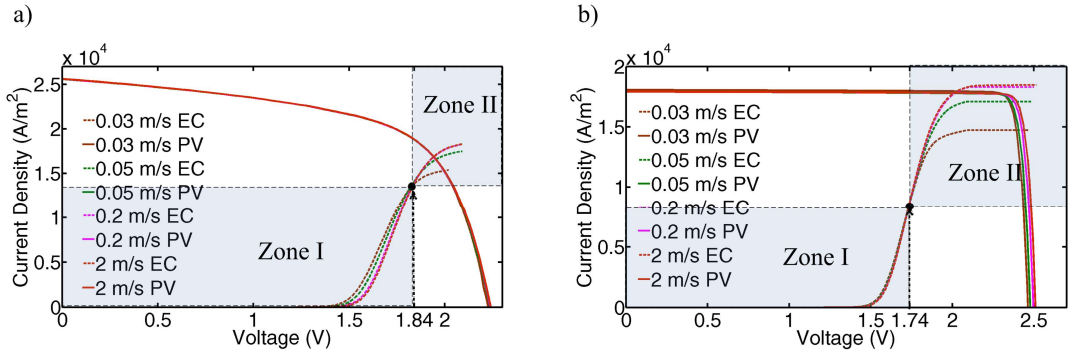

Fig. S.3 The characteristic *J-V* curves for a) aSi-ucSi-ucSi triple junction thin film Si based (C = 450), and b) GaInP-GaAs dual junction III-V based (C = 180) IPEC devices, with varying flow velocities of the water. The black dots show the intersection region of the EC curves, left of which lies the operating zone I and right of which lies the operating zone II.

For flow velocities below 0.2 m/s, we can see noticeable differences in the temperature of the EC component of the device. Due to the higher temperatures at low flow velocities, the *J-V* curves shift left with decreasing flow rates leading to decreased overpotentials. However, zone II is not governed by the temperature effect but, in turn, by the mass transport limitations which are alleviated at higher flow rates. This causes the EC's saturation current to increase at high flow rates, a trend opposite to that observed in zone I.

S.2 Degradation analysis

a. III-V based integrated device

For reference case I, the STH efficiency and operating current density curves for the high and low water flow velocities crosses over after 11.5 years. However, for reference case II (the GaInP-GaAs based case), the crossover never happens due to no shift of the location of the operating points as they always lie in operational zone II. This is evident from Fig. S.4a, where we see that the operating points never cross over to the other side of the zonal intersection point (black dot). However, for both cases, the distance between the two flow rate curves decreases (shown in Fig. S.4b) with time, indicating the diminishing benefit of operating at higher flow rates.

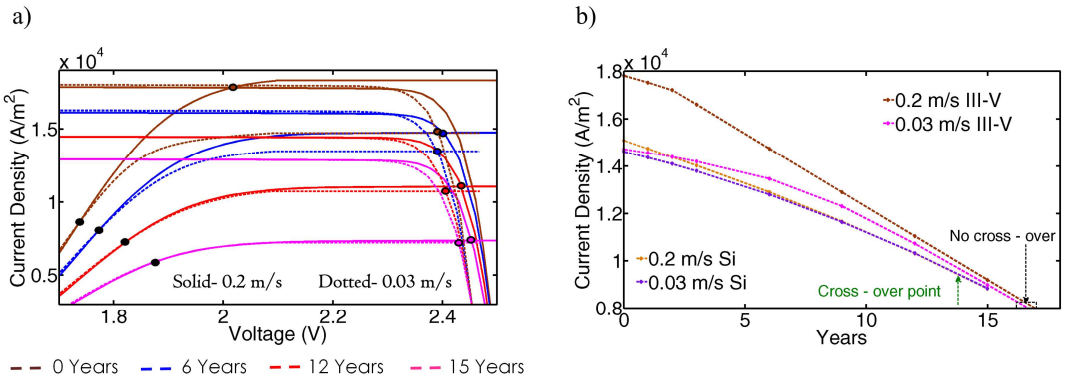

Fig. S.4 The plots showing a) characteristics curves for GaInP-GaAs dual junction PV based IPEC device at C = 180 suns for varying operational years, and b) current density profiles for a III-V based device at C = 180 and a thin film Si based device at C = 450, with increasing operational years.

It is also noted from Fig. S.4a that the operation point of the 0.03 m/s case for the initial operation coincides with the 6 years degraded curves for 0.2 m/s, implying that by varying the flow velocity the initial operating current density for 0.03 m/s can be maintained constant at least for up to 6 years. For finding the appropriate flow controlling profile for stabilizing the output, we plot the output variation for different flow rates for 6 years in Fig. S.5. The required stabilized output (orange) curve is then used to find the appropriate flow rate to maintain the same current density. The resulting controlling profile is presented in the manuscript in the Fig. 4b. 2-axis interpolation (current versus years for different flow rates, and current versus flow rates for different years) is used to obtain the controlling flow profile to achieve a stabilized output.

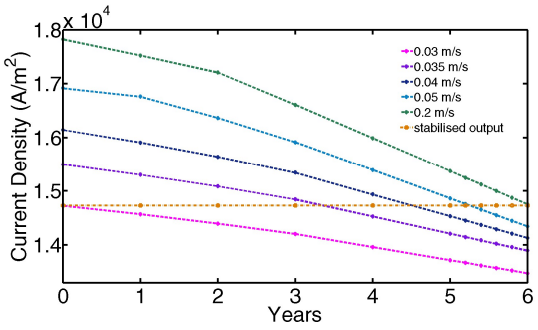

Fig. S.5: The variation of the operating current density for GaInP-GaAs dual junction PV based IPEC device (reference case II) at C = 180 for varying operational years and for different water flow velocities.

b. PV-only degradation analysis and EC-only degradation analysis

The characteristics *J-V* curves for the cases where only the EC components are allowed to degrade and for the case when only the PV components are allowed to degrade are presented in Fig. S.6.

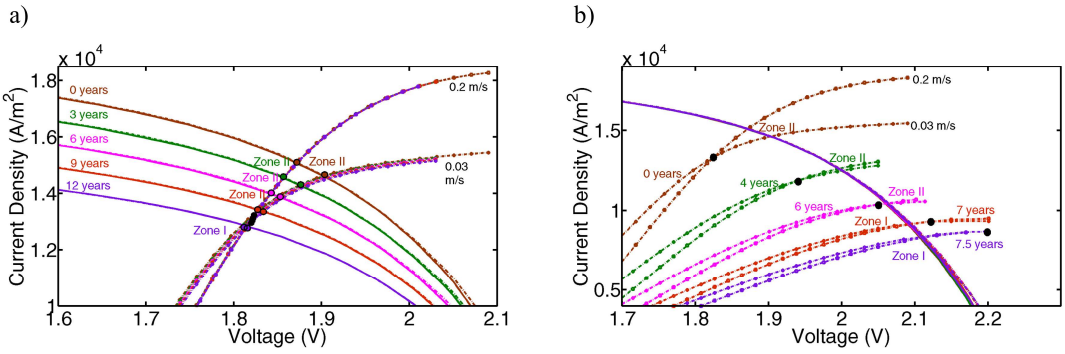

Fig. S.6: The characteristics *J-V* curves for thin film Si PV based IPEC device (reference case I) at C=450 for varying operational years for a) the only-PV degradation case, and b) the only-EC degradation case.

For the PV only degradation case, the EC *J-V* curves for the different years overlap (more or less) on top of each other. Though for 0.03 m/s, the noticeable temperature difference of the EC component still leads to a minimal separation of the *J-V* curves. The intersection points for low and high flow rate EC curves, which decide the demarcation of the zone I and II, are scattered around 1.82 V. All the operating points for the integrated device for the years between 0 to 9 lie on the right side i.e. operational zone II. It is only for the 12th year that the operating points shift

to zone I and this is where the cross-over takes place for the performance plot showing comparison of low and high flow rate, i.e. for Fig. 4b.
For the EC only degradation case, the shift of the operating points from zone II to zone I happens between years 6 and 7 and, hence, the cross-over point shown in Fig. 4b lies at 6.15 years. When only the EC components are allowed to degrade, the PV curves for varying years all lie on top of each other as shown in Fig. S.6b. The EC curves move to lower current densities on the PV curve, and the operating point (shown with black dots) smoothly shifts from zone II to zone I.

S.3 Irradiation variation analysis

The characteristic *J-V* curves for daily irradiation variation analysis (20-140%) for the two water inlet flow velocities of 0.03 m/s and 0.2 m/s are shown below.

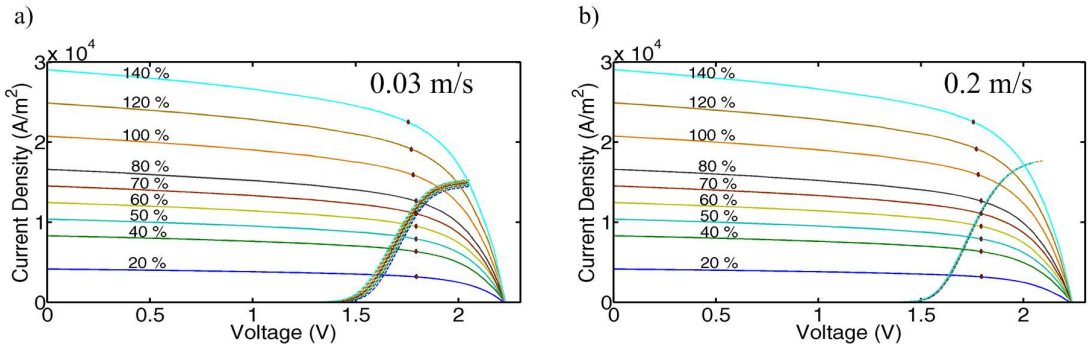

Fig. S.7: The characteristic *J-V* curves for the thin film Si based IPEC device (reference case I) with varying irradiation levels for a) 0.03 m/s and b) 0.2 m/s water flow inlet velocity with C=450 and F=1. The MPP of the PV component is shown by red circles.

The exemple reference irradiation profile for understanding the benefits of water flow rate controlling is presented in Fig. S.8.

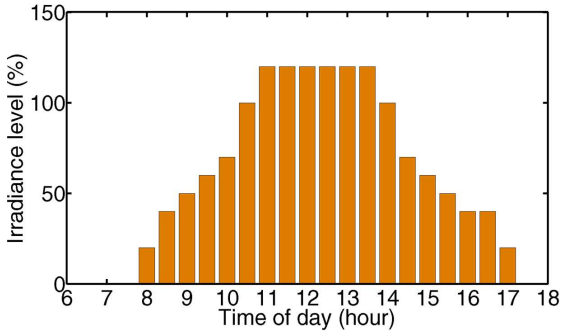

Fig. S.8: The exemplary reference irradiation profile used for the analysis of Fig. 6a and 6b.

REFERENCES:

1 M. Dumortier, S. Tembhurne and S. Haussener, *Energy Environ. Sci.*, 2015, **8**, 3614–3628.
2 F. Fouda-Onana, in *2nd international workshop on durabiltiy and degradation issues in PEM electrolysis cells and its components*, 2016.
3 S. Tembhurne and S. Haussener, *J. Electrochem. Soc.*, 2016, **163**, 988–998.
4 S. Tembhurne and S. Haussener, *J. Electrochem. Soc.*, 2016, **163**, 999–1007.